INSTITUTE OF PHYSICS PUBLISHING JOURNAL OF PHYSICS D: APPLIED PHYSICS

J. Phys. D: Appl. Phys. **38** (2005) 1107–1111 doi:10.1088/0022-3727/38/8/001

Pinning and depinning mechanism of defect dipoles in PMnN–PZT ceramics

BaoShan Li[1], GuoRong Li[1], QingRui Yin[1], ZhiGang Zhu[1], AiLi Ding[1] and WenWu Cao[2,3]

[1] State Key Lab of High Performance Ceramics and Superfine-Microstructure, Shanghai Institute of Ceramics, Chinese Academy of Science, Shanghai 200050, People's Republic of China
[2] Materials Research Institute, Pennsylvania State University, University Park, Pennsylvania 16802, USA
[3] Department of Physics and Materials Science, City University of Hong Kong, Kowloon, Hong Kong, People's Republic of China

E-mail: piezolbs@yahoo.com.cn (GuoRong Li)

Received 1 December 2004, in final form 31 December 2004
Published 1 April 2005
Online at stacks.iop.org/JPhysD/38/1107

Abstract
The frequency and temperature dependences of the hysteresis loops in $Pb[(Zr_{0.52}Ti_{0.48})_{0.95}(Mn_{1/3}Nb_{2/3})_{0.05}]O_3$ ceramics have been investigated. The polarization-field hysteresis curves show 'pinched' shapes at room temperature and higher frequencies, whereas they display normal square-like loops at 200°C and frequencies lower than 10 mHz. Critical ferroelectric features such as the coercive field, polarization and internal bias field show a strong frequency or temperature dependence. The close relations between the P–E loops and the applied frequency and temperature indicate that the defect dipolar moment may change its magnitude with variation of the frequency or temperature. Comparing with the intrinsic depinning procedure induced by the changes in the distribution of defect dipoles, we provide new evidence for an extrinsic depinning mechanism of the defect dipoles in the bulk ceramics.

1. Introduction

The spontaneous polarization in ferroelectric materials can be reversed when a strong electric field is applied opposite to the polarization direction, and this reversibility can be utilized to store data in ferroelectric devices such as ferroelectric nonvolatile memories [1–3]. For this reason, intensive studies have been carried out to reveal the true nature of the switching characteristics. Hysteresis loops are frequently used to determine the ferroelectric properties of materials such as the remnant polarization (P_r), spontaneous polarization (P_s), and coercive field (E_c). These ferroelectric parameters are very sensitive to doping effects. For instances, increasing the oxygen vacancies introduces space charges for acceptor doping [4], which restricts the domain motion and produces a slim loop, whereas lead vacancies are produced to maintain the charge neutrality for donor doping, which increases the squareness of the P–E hysteresis loop.

Among many ferroelectric materials, the $Pb(Mn_{1/3}Nb_{2/3})O_3$-$PbTiO_3$–$PbZrO_3$ (PMnN–PZT) ferroelectric ceramic, which can be used for either acceptor or donor doping, is of particular interest for high-power piezoelectric devices, such as supersonic vibrators and transformers due to its high mechanical quality factor (Q_m), high planar coupling factor (K_p) and low dissipation factor ($\tan\delta$) [5, 6]. In this research, we studied the P–E curves of PMnN–PZT, which shows a 'pinched' shape similar to that of the antiferroelectric ceramics (double loops). To study the origin of these phenomena, the frequency and temperature dependences of the hysteresis loops have been studied.

Various mechanisms have previously been proposed to explain the observed phenomenon. An electrically induced antiferroelectric–ferroelectric transition [7] or an electrically induced paraelectric–ferroelectric transition [8] is unlikely due to the high d_{33} value of about 300 pC N^{-1} in this ceramic system after applying dc polarization. Carl and Hardtl [9] attributed the constricted hysteresis loops to an internal bias field and

observed the disappearance of the distortion of the hysteresis loop in PZT after repeated cycling. Pan *et al* [10] also observed this loop distortion disappearance, and they attributed it to the ionic compensation of oxygen vacancies by electrons injected into the ceramic surface. Some researchers suggest that the constriction is probably related to defect dipoles, which occur near the domain boundary formed by the combination of oxygen vacancies with doped ions at the B-sites. Defect dipoles, sometimes called complex defects, which are formed by acceptor atoms and oxygen vacancies, act as pinning points for the domain motion and result in a constricted loop [11–14]. A bipolar electric field or dc poling can induce the ferroelectric domain depinning process [15]. On the other hand, the absence of complex defects makes the domains more mobile when donor atoms are added [14]. If a combination of acceptors and donors is used, the hysteresis loop resembles that of the undoped material when the acceptor concentration is equal to the donor concentration [16].

In this investigation, the frequency and temperature dependences of polarization-field loops have been studied for PMnN–PZT ceramics near the morphotropic phase boundary (MPB). A qualitative model is proposed to explain the pinning and depinning mechanisms of the defect dipoles.

2. Experimental procedure

The ceramic investigated in this study is $Pb[(Zr_{0.52}Ti_{0.48})_{0.95}(Mn_{1/3}Nb_{2/3})_{0.05}]O_3$. The raw materials, including PbO, $MnCO_3$, Nb_2O_5, ZrO_2 and TiO_2, were wet mixed by ball milling in distilled water for 18 h and then calcined at 850°C for 2 h in an alumina crucible. The re-milled powder was pressed into discs of 12 mm in diameter and 2 mm thickness under 200 MPa. The specimens were sintered at 1220°C for 1 h, under a PbO-rich atmosphere to minimize the lead loss during sintering. The thickness of the specimens was reduced to 0.7 mm by grinding, and silver electrodes were printed onto the two flat surfaces; the specimens were fired at 740°C for 20 min. The temperature dependence of the P–E curves was obtained using a computer-controlled virtual-ground circuit (Radiant Technologies RT66A unit). Due to the retention and relaxation, the loops were usually not closed. The frequency dependence of the hysteresis loops was obtained using a conventional Sawyer–Tower circuit and recorded on a Nicolet 214 digital oscilloscope. A sine-wave electric field of 40 kV cm^{-1} was applied on the samples in the frequency range from 10 mHz to 20 Hz. The specimen was reduced to 0.3 mm in thickness, and then the x-ray photoelectron spectrum (Microlab MKII, VG, UK) was recorded to observe the binding state of the oxygen in the specimens.

3. Results and discussion

The frequency dependence of the hysteresis loops was investigated in the range 10 mHz to 20 Hz, as shown in figure 1 and table 1. When a sine electric field of 20 Hz was applied on the specimen, the pinched shape of the P–E curve was observed as shown in figure 1. There was an alleviation of the pinched shape to some degree with decreasing frequency, and a square-like loop was observed at 10 mHz. The process is reversible. The results from table 1 show that decreasing the

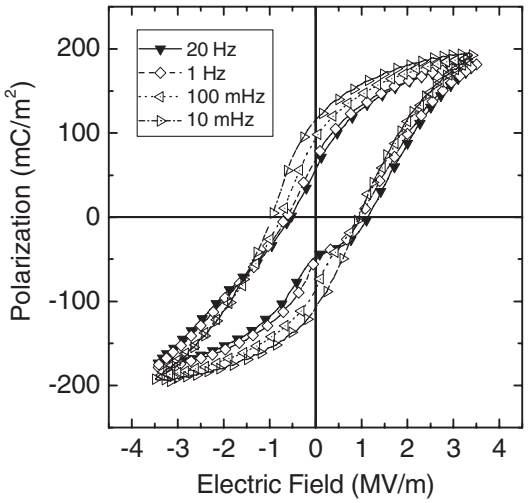

Figure 1. Frequency dependence of the hysteresis loops of PMnN–PZT ceramics.

Table 1. Frequency dependence of the ferroelectric properties of PMnN–PZT ceramics.

Frequency (Hz)	Remnant polarization, P_r (mC m^{-2})	Coercive field, E_c (MV m^{-1})	Internal biasing field, E_i (MV m^{-1})
20	50.9	0.822	0.29
10	55.9	0.849	0.28
1	61.9	0.786	0.18
0.1	87.5	0.826	0.075
0.01	113.7	0.92	∼0

frequency of the applied electric field induces an increase in the coercive field of about 12% and an increase in the remnant polarization of 123%. In the meantime, the internal biasing field, defined as the half-sum of the critical switching fields on the ferroelectric hysteresis loops, decreases to zero with frequency decreasing down to 10 mHz.

Figure 2 shows the temperature dependences of the hysteresis loops for the PMnN–PZT ceramic from room temperature to 200°C. The effect of increasing the temperature on the hysteresis loops has a tendency similar to that of decreasing the frequency. The remnant polarization increases noticeably when the temperature is increased and the square-like loop can be seen when the experimental temperature reaches 200°C. The inset of figure 2 shows the loop for the as-fired specimen at room temperature. Compared with the loop of the naturally aged specimen, it appears much less pinched.

The occurrence of the pinched shape at room temperature and higher frequencies and the disappearance of such distortion at a high temperature and very low frequencies, as shown in figures 1 and 2, show that the constricted shape may be due to charged defects instead of the internal stress because the effect induced by the internal stress does not depend on the frequency. It is highly probable that the defects are interacting with domain walls to induce a pinched hysteresis loop. As far as the PMnN–PZT ceramic is concerned, bivalent Mn and pentavalent Nb with a double doping level substitute for tetravalent Zr or Ti, producing equal amounts of oxygen vacancies and lead vacancies. It is well known that A-site

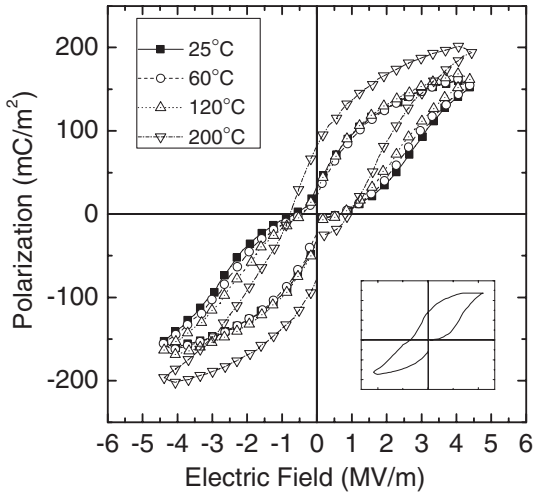

Figure 2. Temperature dependence of the hysteresis loops of PMnN–PZT ceramic (aged in air for several days). The inset shows the P–E loop of the as-fired specimen at room temperature.

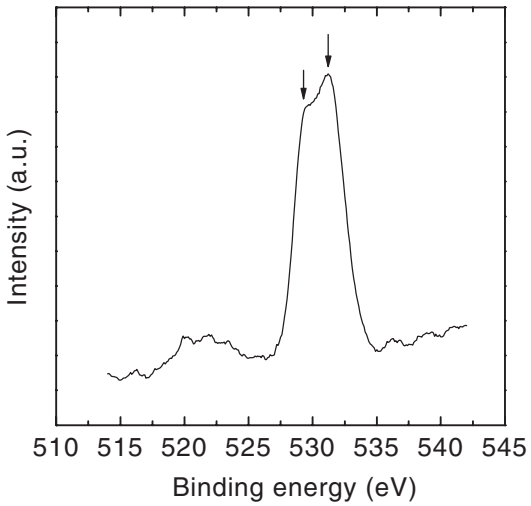

Figure 3. XPS analysis of the photoemission spectra of O1s.

vacancies make the domain walls more mobile, whereas the oxygen vacancies trapped on the domain walls reduce the 90° domain re-orientation and increase the mechanical quality factor (Q_m) [17, 18]. A high Q_m value of 1300 for the PMnN–PZT ceramic suggests that Pb vacancies cannot completely compensate for O vacancies. On the other hand, oxygen vacancies can also be easily created by a loss of oxygen from the crystal lattice at a low oxygen partial pressure or during sintering at high temperatures. Moreover, the complex defects arising from a combination of Nb^{5+} and lead vacancies, i.e. $Nb_{Ti}^{\cdot} \cdot V_{Pb}''$, play an insignificant role regarding the characteristics of the PMnN–PZT. The XPS spectra of the O1s provides another proof of the presence of the oxygen vacancies as shown in figure 3. The peak at 529.4 eV corresponds to O in the perovskite lattice, while the peak at 531.2 eV is indicative of the unsaturated state of the O ion, i.e. $(-2 + x)$ valence. The latter component is therefore related to oxygen vacancies [19]. The charged oxygen vacancies associated with the acceptor impurities will form defect dipoles, and these defect dipoles are attracted to the domain boundaries. Defect dipoles act as pinning points for the 90° domain wall motion and the pinched shape of the P–E loop can be explained by taking into account the pinning effect of these defect dipoles. On the other hand, the 'hard' character (high Q_m value) of the PMnN–PZT ceramic and the presence of the peak at 531.2 eV in O1s spectra suggest the existence of excessive oxygen vacancies that makes the postulation of completely reciprocal compensation of lead and oxygen vacancies proposed by Atkin and Fulrath [16] questionable.

In crystals, the defect moments can be qualitatively described as

$$\Delta\mu = \Delta\mu_d + \sum q_i \Delta_i x_i, \tag{1}$$

where $\Delta\mu_d$ is the variation of dipolar moments in defects and Δx_i is the displacement of the electric charges, q_i, induced by the defects. If the defect dipoles adopt the same orientation and the interaction between them can be ignored, the variation of the macro-polarization is

$$\Delta P = N\Delta\mu, \tag{2}$$

where N is the concentration of the defects. From the internal energy calculation of the crystals, the equivalent electric field caused by the defects is [20]

$$E_d = \frac{\Delta P}{\varepsilon\varepsilon_0}, \tag{3}$$

where ε_0 is the vacuum permittivity and ε the permittivity of the defect-free crystals. Therefore, the equivalent field is more likely an auxiliary bias field added onto the ideal crystals, and this field interacts with the internal field to produce an effect on the domain switching.

It can be concluded from figure 2 that the oxygen vacancies gradually adjust their positions within the six possible locations. The appropriate orientation of the defect dipole may be parallel or antiparallel to the spontaneous polarization, depending on the equilibrium between the electric energy and elastic energy [21]. Electron paramagnetic resonance (EPR) experiments [22] and theoretical modelling [23] suggest that defect dipoles tend to align along the spontaneous polarization and this is applicable for the PMnN–PZT ceramic. We deduce that the polarization of the defect dipoles is parallel to the spontaneous polarization due to a minor increase in the coercive field at the depinning state as shown in table 1. According to [21], the internal bias field is equivalent to the energy difference between the two poling directions (positive and negative electric fields). Hence, the depinning process may be treated as the annihilation of the defect dipoles or the significant weakening of the sorts of defect dipoles which decrease the remnant polarization.

Recently, the depinning mechanisms of the defect dipoles during the fatigue process have attracted more researchers. Lente and Eiras [24, 25] believed that when the alignment between the switchable domains with the defect dipoles passed from parallel to perpendicular, the interaction between them is null and the coercive field returns to the defect-free case. Kohli *et al* [15] considered that the dipinning process could be imagined as a multiple knocking of domain walls on defect dipoles, which leads to a re-distribution of defects. However, these explanations aim at the intrinsic depinning procedure and may not apply to our experiments that were carried out under

different conditions. First, there are no excessive reversals of the domains. Second, the same unsaturated loop can be observed when the applied frequency is decreased and then increased back. Repeated occurrences of the pinning effect with the variation of frequency suggest that annihilation of the defect dipoles did not happen, for it is hard to imagine how they can be re-activated after neutralization. In addition, it is reasonable that the activation energy for rotating the defect diploes in PMnN–PZT is much higher [21, 26]. Therefore, it is difficult for the defect dipole to re-orientate either at 200°C or with 10 mHz. Hence, a good explanation for the depinning procedure is that the defect dipoles which are in the direction opposite to the polarization are significantly suppressed, while the defect moments which are in the same direction as the polarization will be lengthened at a very low frequency or higher temperature. Hence, the defect dipolar moment, μ_d, can be qualitatively estimated as a function of the electric field (E), temperature (T) and frequency (f), which is expressed in the following way:

$$\mu_d = \mu_d(E, T, f). \tag{4}$$

μ_d varies with the applied frequency and temperature, resulting in the pinning or depinning process of the hysteresis loop.

We have calculated the activation energy of conductivity according to the Arrhenius equation, $\sigma = \sigma_0 \exp(-E_a/KT)$, as shown in figure 4. The dc conductivity plot gives an activation energy of 1.13 eV at temperatures above 370°C, which is close to the commonly accepted value for an oxygen vacancy [27]. Thus, oxygen vacancies may undergo different states in three different temperature ranges: (1) steady state of the oxygen vacancies with electric field (0–200°C), (2) unstable state of the oxygen vacancies (200–370°C) and (3) oxygen vacancies participating in ionic conductivity (above 370°C).

It is known that the fast pulse mode is used in the RT66A testing system. Hence, the applied field frequency in figure 2 is much higher than that in figure 1, and therefore a very severely pinched loop is observed. A schematic picture as shown in figure 5 is then proposed to explain the pinning and depinning mechanisms of the defect dipoles. Parallel orientation with respect to the polarization is preferred from figures 5(*a*) and (*b*) as defect dipoles are energetically favoured at the original state and the reverse defect moments are suppressed at a low frequency or high temperature as shown in figures 5(*d*) and (*f*). However, only minor suppression of the reverse defect moments occurs in figure 5(*c*) at high frequencies and there is almost no suppression of the defect dipoles at room temperature in figure 5(*e*) due to the very fast pulse mode used.

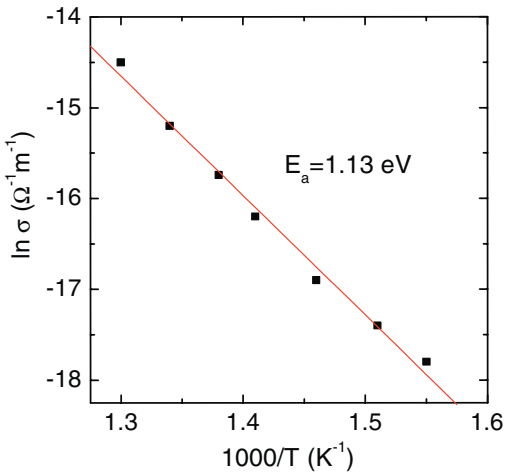

Figure 4. Arrhenius plot for dc conductivity characteristics obtained by least-square linear fitting.

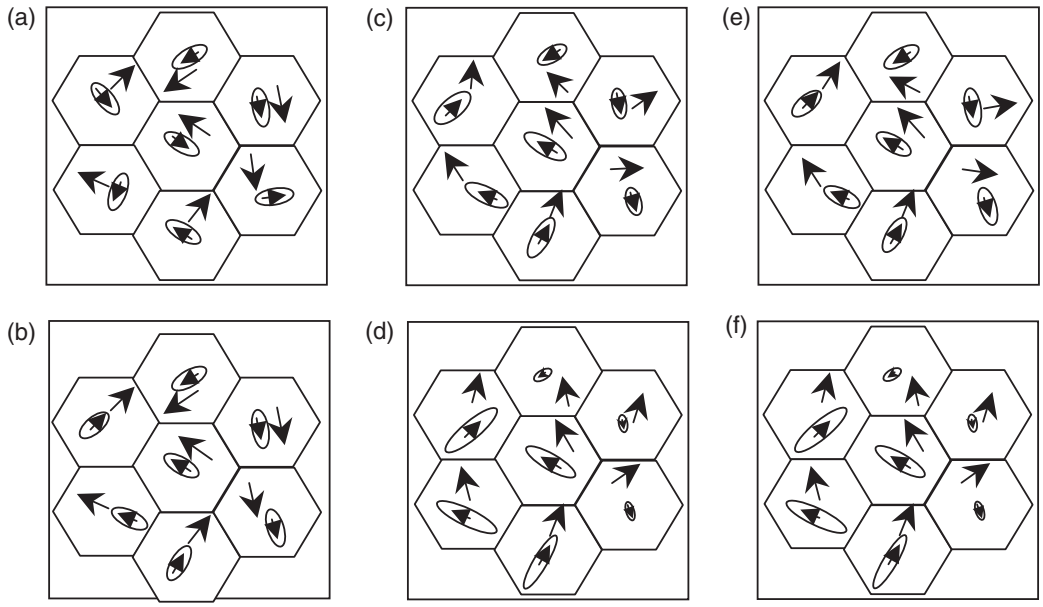

Figure 5. A schematic illustration for the pinning and depinning process of the P–E curves. (*a*) As-fired state, (*b*) original state, (*c*) high frequency (Sawyer–Tower), (*d*) low frequency (Sawyer–Tower), (*e*) low temperature (RT66A) and (*f*) high temperature (RT66A). The large arrows represent the spontaneous polarization, and the arrows in ellipses refer to the orientation of the defect dipoles. The elliptical length represents the magnitude of the defect dipolar moment. 'Original state' refers to the naturally aged specimen (in air for several days), and the P–E loops shown all begin with this state. The states of the defect dipoles in (*c*)–(*f*) occur at high electric fields.

4. Conclusions

In this work, the frequency and temperature dependence of the hysteresis loops in the PMnN–PZT piezoelectric system were investigated to reveal the causes for the constriction in the P–E curves. Our results suggest that defect dipoles are the primary cause, which preferably orientate themselves along the spontaneous polarization, and they induce the orientations of the domains along themselves at a low electric field, resulting in the pinched shape of the hysteresis loops at room temperature and higher frequencies. On the other hand, the pinched degree is primarily determined by the change in the defect moment, which is affected by the temperature and frequency.

Therefore, the extrinsic depinning process can be considered as the suppression of the negative defect moments and augmentation of the positive ones.

Acknowledgments

The authors would like to acknowledge financial support of the National 973 Project of China (NO 2002CB13307) and the Hong Kong RGC under Grant No City U 1056/02P.

References

[1] Scott J F and Paz De Araujo C A 1989 *Science* **246** 1400
[2] Haertling G H 1999 *J. Am. Ceram. Soc.* **82** 797
[3] Yin J H and Cao W W 2002 *Appl. Phys. Lett.* **79** 4556
[4] Jiang Q Y, Subbarao E C and Cross L E 1994 *J. Appl. Phys.* **75** 7433
[5] Osamu I, Kaoru S and Yoichi M 1999 *Japan. J. Appl. Phys.* **38** 5531
[6] Tomoaki F, Hiroshi S and Masatoshi A 1999 *Japan. J. Appl. Phys.* **38** 3596
[7] Shirane G, Sawaguchi E and Takagi Y 1951 *J. Phys. Soc. Japan* **6** 333
[8] McQuarrie M 1955 *J. Am. Ceram. Soc.* **38** 444
[9] Carl K and Hardtl K H 1978 *Ferroelectrics* **17** 473
[10] Pan M J, Park S E, Park C W, Markowski K A, Yoshikawa S and Randall C A 1996 *J. Am. Ceram. Soc.* **79** 2971
[11] Scott J F and Dawber M 2000 *Appl. Phys. Lett.* **76** 3801
[12] Scott J F and Pouligny B 1998 *J. Appl. Phys.* **64** 1547
[13] Li B S, Zhu Z G, Li G R, Yin Q R and Ding A L 2004 *Japan. J. Appl. Phys.* **43** 1458
[14] Wu L, Wei C, Wu T and Teng C 1983 *J. Phys. C: Solid State Phys.* **16** 2803
[15] Kohli M, Muralt P and Setter N 1998 *Appl. Phys. Lett.* **72** 3217
[16] Atkin R B and Fulrath R M 1971 *J. Am. Ceram. Soc.* **54** 265
[17] Yoon S J, Joshi A and Uchino K 1997 *J. Am. Ceram. Soc.* **80** 1035
[18] Kim J S, Kim S J, Kim H G, Lee D C and Uchino K 1999 *Japan. J. Appl. Phys.* **38** 1433
[19] Jovalekić Ĉ, Pavlović M, Osmokrović P and Atanasoska L J 1998 *Appl. Phys. Lett.* **72** 1051
[20] Yin Z W 2003 *Physical Principles of the Dielectric* (China: Science Publications)
[21] Arlt G and Neumann H 1988 *Ferroelectrics* **87** 109
[22] Warren W L, Dimos D, Pike G E, Vanheusden K and Ramesh R 1995 *Appl. Phys. Lett.* **67** 1689
[23] Lohkamper R, Neumann H and Arlt G 1990 *J. Appl. Phys.* **68** 4220
[24] Lente M H and Eiras J A 2002 *J. Appl. Phys.* **92** 2112
[25] Lente M H and Eiras J A 2001 *J. Appl. Phys.* **89** 5093
[26] Ren X B 2004 *Nature Mater.* **3** 91
[27] Chan N H, Sharma R K and Smyth D M 1982 *J. Am. Ceram. Soc.* **65** 167